

ORIGINAL ARTICLE

Open Access



# Biochemical composition of soil organic matter physical fractions under 32-year fertilization in Ferralic Cambisol

Yang Chen<sup>1</sup>, Kailou Liu<sup>2</sup>, Ning Hu<sup>3</sup>, Yilai Lou<sup>4</sup>, Fang Wang<sup>1</sup> and Yidong Wang<sup>1\*</sup> 

## Abstract

Biochemical properties of soil organic matter (SOM) are fundamental for soil fertility and health. However, it is unclear how fertilization regime influences the biochemical compositions and oxidation states of SOM and physical fractions. In this study, this issue was studied under four 32-year amendment regimes: unfertilized control, urea (N), N + calcium dihydrogen phosphate + potassium chloride (NPK), and NPK plus manure (NPKM). Three physical fractions: coarse particulate (> 250  $\mu\text{m}$ , cPOM), fine particulate (53–250  $\mu\text{m}$ , fPOM) and mineral-associated OM (< 53  $\mu\text{m}$ , MAOM) were separated and measured by pyrolysis gas chromatography/mass spectrometry (Py-GC/MS). Compared with the background in 1986, the SOM increased by 10.6%, 14.2%, 23% and 52% in unfertilized control, N, NPK, and NPKM, respectively. The red soil here had not reached carbon saturation, because of the low conversion efficiency (6.8%) from input-carbon to soil organic carbon (SOC). Physical size but not amendment type primarily regulated the SOM molecular composition, with relative selective retention of aromatics and lignin in both the cPOM and fPOM, whereas N-containing compounds (particularly amino-N) were enriched in MAOM due to their high abilities to adsorb soil minerals. The C oxidation state was also mainly dependent on physical size, with the highest value in fPOM. The sources of SOM and its fractions, dominated by microbial-derived compounds (60–90%), were independent of physical size and fertilization. In conclusion, physical size arrangement (proxy of microbial decomposition degree) played a more important role in regulating the SOM biochemical features than initial quality of various amendments.

## Highlights

- Physical size, instead of fertilization, greatly modulated biochemical compositions and oxidation states of SOM.
- Aromatics and lignin were enriched in POM fractions, while N-bearing compounds were abundant in MAOM.
- The red soil here had not reached SOC saturation, due to a low conversion efficiency of 6.8%.

**Keywords** C oxidation state, Lignins, N-containing compounds, Organo-mineral associations, Particulate organic matter, Py-GC/MS

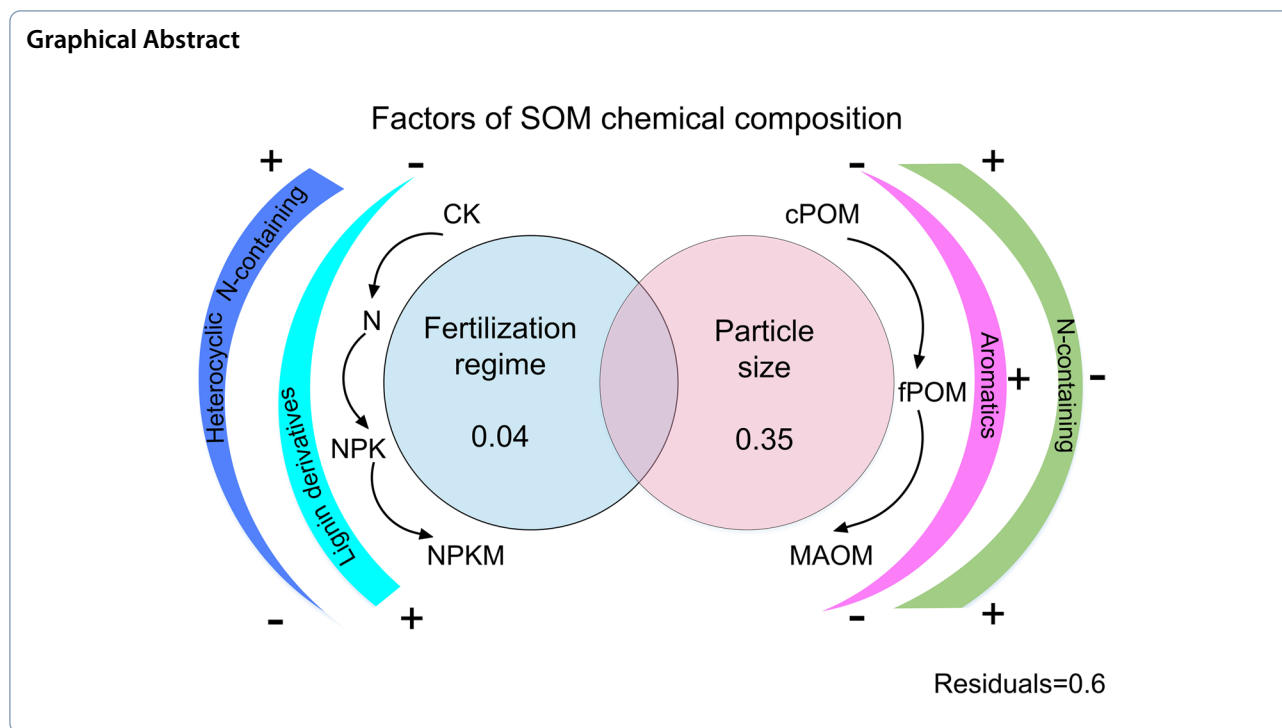
\*Correspondence:

Yidong Wang  
wangyidong@tjnu.edu.cn

Full list of author information is available at the end of the article



© The Author(s) 2023. **Open Access** This article is licensed under a Creative Commons Attribution 4.0 International License, which permits use, sharing, adaptation, distribution and reproduction in any medium or format, as long as you give appropriate credit to the original author(s) and the source, provide a link to the Creative Commons licence, and indicate if changes were made. The images or other third party material in this article are included in the article's Creative Commons licence, unless indicated otherwise in a credit line to the material. If material is not included in the article's Creative Commons licence and your intended use is not permitted by statutory regulation or exceeds the permitted use, you will need to obtain permission directly from the copyright holder. To view a copy of this licence, visit <http://creativecommons.org/licenses/by/4.0/>.



## 1 Introduction

Soil organic matter (SOM) remains fundamental in fertility, plant productivity, biodiversity, eco-environmental sustainability and global climate change (Schmidt et al. 2011; Paul 2016), due to its inherent chemical properties (Lehmann and Kleber 2015). The SOM consists of main biochemical components: aromatics, lignin, lipids, N-containing compounds, phenols, and polysaccharides (Kallenbach et al. 2016; Yan et al. 2022). These biochemical compositions of SOM are mainly regulated by the initial quality of OM input (Kögel-Knabner 2002), microbial decomposition (Simpson et al. 2007; Sokol and Bradford 2019), and organo-organic (Possinger et al. 2020) and organo-mineral associations including aggregation (Totsche et al. 2018; Creamer et al. 2019; Kopittke et al. 2020; Kleber et al. 2021).

There are multiple pools with various composition and functions in SOM (von Lützow et al. 2007). Emerging paradigms suggest that physical isolation (organo-mineral association and occlusions inside of microaggregates) is the principal mechanism for its prolonged persistence (Baldock and Skjemstad 2000; Lehmann and Kleber 2015; Hemingway et al. 2019; Kögel-Knabner and Amelung 2021), and also explains biochemical composition of SOM (Bol et al. 2009; Barré et al. 2018). Particulate OM (>53  $\mu\text{m}$ , POM) and mineral-associated OM (<53  $\mu\text{m}$ , MAOM) are formed by specific processes and localized (spatial arrangement) in various pores and aggregates, and consequently have various persistence (turnover time or residence) and functions (Lützow et al. 2007; Bol et al. 2009;

Lavallee et al. 2020; Schweizer et al. 2021). Globally, the SOM has an average C/N ratio of 12.3 (Cleveland and Liptzin 2007; Cai et al. 2022). The POM group, mostly derived from plant-residue, has C/N ratios of 10–40, whereas the MAOM group, mainly from microbial residues, has C/N ratios of 8–13 (Christensen 2001; Lützow et al. 2007; Kögel-Knabner et al. 2008). The POM group can be further separated into coarse (>250  $\mu\text{m}$ , cPOM) and fine fractions (53–250  $\mu\text{m}$ , fPOM) (Six et al. 2000; Wang et al. 2021), and the fPOM can be separated from cPOM after its disintegration (Six et al. 2000). The biochemical compositions of the cPOM, fPOM and MAOM were reported to be different (Bol et al. 2009). However, fewer studies were available for subtropical areas, where long-term soil formation resulted in partial depletion of clay minerals and relative accumulation of iron and aluminum oxides (Guo et al. 2020; Song et al. 2022b). This composition of the mineral soil phase (enrichments of iron and aluminum oxides) may shift the biochemical composition of SOM and its fractions (Creamer et al. 2019; Kopittke et al. 2020; Kleber et al. 2021; Kögel-Knabner and Amelung 2021) via stronger physical protection, which is different from temperate soils. High microbial activity in wet subtropics induces faster rate of SOM mineralization and higher degree of decomposition compared to temperate zone, especially for POM (Wang et al. 2021). And high microbial activity also affects the SOM oxidation state, while high (less negative) oxidation state indicates lower vulnerability to microbial decomposition (Hockaday et al. 2009; Gunina

et al. 2017). Nevertheless, there is still a knowledge gap on biochemical compositions and C oxidation states of SOM along with the physical size classes in wet subtropical soils.

Fertilization, one key management practice in agro-ecosystems, generally increases the SOM pool, particularly under manure and straw application (e.g., Wang et al. 2015; Wang et al. 2018; Song et al. 2022a), shifts its fractionation, and usually towards more labile features (POM, mainly cPOM) (e.g., Yang et al. 2019; Shah et al. 2021). Among the SOM compounds, the amount of N-containing biopolymers (amino compounds, heterocyclic compounds and others) increases after N fertilization (Hasegawa et al. 2021). In paddy field, however, mineral N and organic amendments all had little influence on biochemical compositions of SOM including the proportion of N-bearing biopolymers (Yan et al. 2022). The aromatics and lignin, residual compounds during decomposition, are more recalcitrant in soils compared with others (Kleber 2010; Steffens et al. 2011) and can be affected by fertilization-induced plant debris and manure input. However, it is still unclear how long-term organic and mineral fertilizations influence the chemistry of SOM.

The objective was to examine the biochemical features of SOM physical fractions under various long-term fertilizations in the Ferralic Cambisol – a typical soil in wet subtropics. We hypothesized that: (i) the biochemical compositions and oxidation states of the SOM were mainly shifted by physical sizes because of their corresponding decomposition degree. The microbial-processed N-containing compounds were enriched in MAOM, and the recalcitrance compounds were retained relatively and selectively in the cPOM and fPOM; and (ii) the various fertilizations also shifted the biochemical compositions of SOM, towards increments in lignin and N-bearing compounds due to the inputs of N-fertilizer, crop debris and manure.

## 2 Materials and methods

### 2.1 Study site and design

This work was conducted in the Jinxian experimental station (28°21' N, 116°10' E) in southern China. The research site was flat and well-drained and was characterized by a humid subtropical monsoon climate. In the current study, the average temperature was 18°C, average precipitation was 1730 mm yr<sup>-1</sup>, frost-free period was 282 d yr<sup>-1</sup> and sunshine duration was 1900–2000 hr yr<sup>-1</sup>. The experimental soils were Ferralic Cambisol (FAO), developed from the quaternary red clay (Zhang et al. 2015; Song et al. 2022a), with a texture of 16% sand, 60% silt, and 24% clay.

Prior to the long-term experiment (before 1986), the area was mainly covered by small trees (that is *Pinus* spp.) till 1960s, and was subsequently was cultivated with soybean (that is *Glycine max* L., C3 plant) and peanuts (that is *Arachis hypogaea*, C3 plant). Since 1986, the field had a double-cropping regime of maize-maize (spring and summer). The

initial 0–20 cm soil properties in 1986 included: bulk density of 1.20 g cm<sup>-3</sup>, soil organic carbon (SOC) of 8.93 g kg<sup>-1</sup>, total nitrogen (TN) of 0.98 g kg<sup>-1</sup>, total phosphorus (TP) of 0.62 g kg<sup>-1</sup>, total potassium (TK) of 11.4 g kg<sup>-1</sup>, and pH 6.0 (Zhang et al. 2015; Yang et al. 2018; Song et al. 2022a).

The formal experiment were started in early 1986. Four fertilization regimes: no fertilizers (control), urea (N), urea plus Ca(H<sub>2</sub>PO<sub>4</sub>)<sub>2</sub> plus KCl (NPK), and NPK plus manure (NPKM) were randomly designed with 3 replicates. The area of every replicate plot was 22.22 m<sup>2</sup>, surrounded by thick cement baffles deep to 1 m. Fertilizers were applied for both maize crops in the following rates: N – 60 kg ha<sup>-1</sup>; NPK – 60 (N), 13 (P) and 50 (K) kg ha<sup>-1</sup>; NPKM – pig manure of 15,000 kg ha<sup>-1</sup> (fresh). The pig manure had dry-weight contents of C (376.1 g kg<sup>-1</sup>), N (33.1 g kg<sup>-1</sup>), P (23.8 g kg<sup>-1</sup>) and water of 71.6%. In each maize season, 100% P and 100% manure were used as base fertilizers, while 100% K and 50% N were applied for 1 week following with the sowing as top dressings and 50% N was further applied for 2 weeks after sowing (Song et al. 2022a).

In the double-cropping system, the spring maize was grown from mid-April to early July, while the summer maize was cultivated from late July to early November. Both types of the maize was seeded 50 cm apart in rows with a line interval of 30 cm. The maize hybrid variety changed approximately every 5-year to improve grain production in the region. The pesticides and herbicides were used as required. The yield and straw biomass (besides 5–10 cm stubble) were recorded yearly. The other agricultural practices including tillage were the same for all the fertilizations (Zhang et al. 2015; Song et al. 2022a).

### 2.2 Soil sampling and physical fractionation

A composite soil (homogenized from 3 points) in each plot was sampled at 0–20 cm layer 2 weeks after maize-harvest in November 2017. Potential impacts of fertilization and growth condition were minimized by the specific selection of sampling time. Bulk density was measured according to the core cutter method (100 cm<sup>3</sup>) in the middle of the soil layer. All soil samples were air-dried in room and then passed through 2-mm sieve. All visible gravels, plant residues (shoots and roots) and fauna were removed before sieving procedure.

Three physical sizes (>250, 53–250, <53 μm) were isolated using wet-sieving approach. In brief, 25 g dry soil, 25 glass beads and 60 mL deionized water were placed in a 100 mL volume plastic bottle. The plastic bottle was oscillated for 1 h with 180 r min<sup>-1</sup>. The soil slurry was sieved using a 250-μm mesh screen. The retained part on the sieve was collected into an aluminum box and dried to a constant weight at 60°C, which presented cPOM (>250 μm).

The soil suspension through the 250- $\mu\text{m}$  mesh screen was dried at 60°C and then moved into a 100 mL plastic bottle, with 25 glass beads and 60 mL 5 g L<sup>-1</sup> (NaPO<sub>3</sub>)<sub>6</sub> added. The soil suspension was oscillated with 180 r min<sup>-1</sup> for 18 h and then sieved with 53- $\mu\text{m}$  mesh screen. The retentate on sieve was collected and dried to a constant weight at 60°C, which presented the fPOM (53–250  $\mu\text{m}$ ). The soils through the 53- $\mu\text{m}$  mesh screen were also dried at 60°C, which presented the MAOM (<53  $\mu\text{m}$ ) (Yan et al. 2022).

The contents of SOC and TN in bulk soil as well as three physical fractions (cPOM, fPOM and MAOM) were analyzed using an elemental analyzer (PerkinElmer 2400 II, USA). The C/N referred to SOC/TN. The SOM content was estimated from the SOC content using a conversion factor of 1.724.

### 2.3 Determination of SOM biochemical composition

The biochemical compositions of straw, pig manure, and SOM as well as its fractions were analyzed using the pyrolysis-gas chromatography/mass spectrometry (Py-GC/MS) (Pyrolyzer, PY-2020iD, Frontier Laboratories Ltd., Japan; GC/MS, QP-2010Ultra, Shimadzu, Japan). Because the Py-GC/MS is useful for characterizing biochemical composition of OM. In brief, 5 mg fully ground bulk soil or fraction, with 1 mL 25% tetramethylammonium hydroxide for derivatization, was laid in white-gold boat, which was freely fallen in the quartz pyrolysis cracking tube (600°C). Following the quick pyrolysis, the pyrolysis compounds were delivered to the GC with a temperature of 300°C on interface and a split injection ratio of 100:1 (0.8 mL He min<sup>-1</sup> flow rate). The compounds were separated in a DB-5 column (30 m  $\times$  0.25 mm  $\times$  0.25  $\mu\text{m}$ ). The GC had a temperature schedule of 40°C for 3 min, 10°C min<sup>-1</sup> to 260°C, followed by 15°C min<sup>-1</sup> to 300°C (final temperature) for 5 min. The MS worked at 70 eV in EI mode (source temperature of 200°C) and had a mass/charge scan range of

29–500. The pyrolysis compound peaks are analyzed and identified according to the National Institute of Standards and Technology (NIST) library database (2011 Edition).

A total of 368 biochemical components were identified and were classified into 10 groups according to chemical and analytical similarities (Pascaud et al. 2017; Becker et al. 2019; Chen et al. 2019; Yan et al. 2022): lipids, monocyclic-, polycyclic-aromatics, phenolics, polysaccharides, lignins, amino N-bearing compounds, heterocyclic N-bearing compounds, other N-bearing compounds and unidentified compounds. During the pyrolysis by Py-GC/MS, amino acids were transformed by mistake easily into the imidazoles, indoles, pyridines, pyrroles, pyrazines, and nitriles, most commonly (Schulten and Schnitzer 1997; Becker et al. 2019; Yan et al. 2022). Therefore, the above six compounds were unified into amino N-containing compounds. Unspecified compounds are compounds containing halogen atoms (Br, I, Cl) and complex functional groups.

### 2.4 Sources, stability and oxidation state of SOM

All the pyrolysis products were classified into 3 sources: microbial-derived, plant-derived, and mixed (plant + microbial) (Schellekens et al. 2017; Angst et al. 2021). The lignins, long-chain lipids (> 18C), polysaccharides, phenolics, amino N-bearing (indoles), and heterocyclic N-compounds (pyrazines) were mainly classified as the plant-derived fraction. The aromatics, short-chain lipids (< 16C), amino N-bearing compounds (nitriles, pyridines, pyrroles), and other N-bearing compounds were classified as microbial-derived. The multiple origins compounds were unspecified and some were lipids (16C–18C) (Stewart et al. 2011; Barré et al. 2018; Becker et al. 2019; Chen et al. 2019; Yan et al. 2022). The atomic H/C, O/C, and N/C ratios and oxidation state were estimated according to the Eqs. (1–4), respectively (Hockaday et al. 2009; Kleber 2010).

$$H/C = \sum \left[ (H_n \times 1/C_{P_{m-w}}) \times C_{P_p} \right] \times 12 / \sum \left[ (C_n \times 12/C_{P_{m-w}}) \times C_{P_p} \right] \quad (1)$$

$$O/C = \sum \left[ (O_n \times 16/C_{P_{m-w}}) \times C_{P_p} \right] \times 12 / 16 / \sum \left[ (C_n \times 12/C_{P_{m-w}}) \times C_{P_p} \right] \quad (2)$$

$$N/C = \sum \left[ (N_n \times 14/C_{P_{m-w}}) \times C_{P_p} \right] \times 12 / 14 / \sum \left[ (C_n \times 12/C_{P_{m-w}}) \times C_{P_p} \right] \quad (3)$$

$$\text{Oxidation state} = 3 \left\{ \sum \left[ (O_n \times 16/C_{P_{m-w}}) \times C_{P_p} \right] - 8 \sum \left[ (H_n \times 1/C_{P_{m-w}}) \times C_{P_p} \right] \right\} / 2 \sum \left[ (C_n \times 12/C_{P_{m-w}}) \times C_{P_p} \right] \quad (4)$$

where the N/C, O/C, and H/C are atomic ratios; the  $H_n$ ,  $C_n$ ,  $N_n$ , and  $O_n$  are atomic numbers of H, C, N, and O in every pyrolysis product, respectively; the numbers of 1, 12, 14, and 16 refer to atomic masses of H, C, N, and O, respectively; the  $C_{p_{m-w}}$  represents the pyrolysis molecular-weight; the  $C_{p_p}$  refers to mass contribution of every pyrolysis product to whole SOM.

## 2.5 32-year total input-C from plant residue (root and stubble) and manure

In every replicate plot, the straw biomass and grain yield of the double cropping maize (spring and summer) were separately harvested and dry-weighted. The biomasses of straw and grain were summed as the total aboveground biomass.

The 32-year total plant residue-derived input-C of each replicate plot was calculated based on the Eqs. (5–7).

$$\text{InputC}_{\text{residue}} = \sum \text{Maize}_{\text{root}} + \sum \text{Maize}_{\text{stubble}} \quad (5)$$

$$\sum \text{Maize}_{\text{root}} = \sum B_s \times (1 - W_s) \times R_{r-s} \times C_r \times 85.1\% \quad (6)$$

$$\sum \text{Maize}_{\text{stubble}} = \sum B_s \times (1 - W_s) \times R_{s-s} \times C_s \quad (7)$$

where the  $\text{InputC}_{\text{residue}}$  is the 32-year total input-C from the plant residue (root and stubble) ( $\text{t C ha}^{-1}$ ); the  $\sum \text{Maize}_{\text{root}}$  is the 32-year total root-input-C ( $\text{t C ha}^{-1}$ ) from both the spring and summer maize; the  $\sum \text{Maize}_{\text{stubble}}$  represents the 32-year cumulative stubble-input-C ( $\text{t C ha}^{-1}$ ) from both the spring and summer maize; the  $B_s$  refers to the yearly maize shoot biomass (grain + straw) ( $\text{t C ha}^{-1} \text{yr}^{-1}$ ); the  $\sum B_s$  refers to the 32-year total maize shoot biomass ( $\text{t C ha}^{-1} \text{yr}^{-1}$ ); the  $W_s$  is water content of maize whole shoot (14%); the  $R_{r-s}$  refers to root/shoot ratio of maize in this study field (the control, N, and NPKM, 0.19; and the NPK, 0.29) based on the previous study (Zhang et al. 2015); the  $C_r$  is the C content of dried maize root (45%) (Zhang et al. 2015); the 85.1% refers to the proportion of 0–20 cm root biomass to total root biomass (Li et al. 1992; Liu and Song 2007; Song et al. 2022a); the  $R_{s-s}$  is the average ratio of stubble/shoot biomass of maize in this field (control, 0.036; N, 0.014; NPK, 0.011; and NPKM, 0.018); and the  $C_s$  is the C content of dried maize stubble (45%) (Zhang et al. 2015).

The 32-year total input-C from the pig manure was estimated based on Eq. (8) (Wang et al. 2015).

$$\text{InputC}_{\text{manure}} = M_f \times (1 - W_m) \times C_m \times 32 \quad (8)$$

Where the  $\text{InputC}_{\text{manure}}$  is the 32-year total manure-input-C ( $\text{t C ha}^{-1}$ ); the  $M_f$  is fresh pig manure amendment rate of  $30 \text{ t ha}^{-1} \text{yr}^{-1}$ ; the  $W_m$  refers to the moisture

of fresh manure (71.6%); the  $C_m$  represents C content of dry manure ( $376 \text{ g kg}^{-1}$  dry weight); and the number 32 is the experiment duration.

The 32-year total input-C from both the plant residue and manure was calculated based on the Eq. (9). The SOC stock of 0–20 cm layer was estimated using bulk density and SOC content according to the Eq. (10). SOC sequestration was calculated by the Eq. (11).

$$\text{InputC}_{\text{total}} = \text{InputC}_{\text{manure}} + \text{InputC}_{\text{residue}} \quad (9)$$

$$\text{CS} = \text{SOC} \times \text{BD} \times 20 \quad (10)$$

$$\Delta \text{SOC} = \text{CS}_{\text{treatment}} - \text{CS}_{\text{initial}} \quad (11)$$

where the  $\text{InputC}_{\text{total}}$  is the 32-year total input-C ( $\text{t C ha}^{-1}$ ) from both the plant residue and manure; the CS refers to 0–20 cm SOC stock ( $\text{t C ha}^{-1}$ ); the SOC refers to its content ( $\text{g kg}^{-1}$ ); the BD refers to bulk density (control and N,  $1.31 \text{ g cm}^{-3}$ ; NPK,  $1.3 \text{ g cm}^{-3}$ ; NPKM,  $1.32 \text{ g cm}^{-3}$ ) (Zhang et al. 2015); the number 20 is the 0–20 cm depth,  $\Delta \text{SOC}$  refers to SOC sequestration of the current minus initial C storage ( $\text{t C ha}^{-1}$ ); the  $\text{CS}_{\text{treatment}}$  represents the SOC storage ( $\text{t C ha}^{-1}$ ) of the four treatments; and the  $\text{CS}_{\text{initial}}$  refers to the initial SOC storage in 1986 ( $21.43 \text{ t C ha}^{-1}$ ).

## 2.6 Statistical analysis

The analyses of variance following Tukey's test were carried out in SPSS 26 (SPSS Inc., Chicago, Illinois, USA). The analysis of non-metric multidimensional scaling (NMDS) was conducted on Past 3 (Hammer et al. 2001). The variance partitioning analysis was done based on RStudio (package 'vegan', R Soft Team, 2015). Figures were drawn using the ORIGIN 2018 (Origin Lab Corp., Northampton, USA).

## 3 Results

### 3.1 Mass proportion of physical sizes

The MAOM held >80% of total SOM, and the mass proportion of fPOM was <5% for all treatments (Fig. 1). Compared with the unfertilized control, the NPK amendment increased the mass portion of cPOM by +38.5% and decreased the portion of MAOM by –6.5%. However, the NPKM decreased the cPOM mass by –49% and enhanced the mass portions of fPOM and MAOM by +57% and +7.7%, respectively, compared with the unfertilized control (Fig. 1). By contrast, N treatment had little impact on the mass proportion (Fig. 1).

### 3.2 SOC and total N

Over the 32 years, the unfertilized control, N, NPK, and NPKM amendments increased the SOC contents by



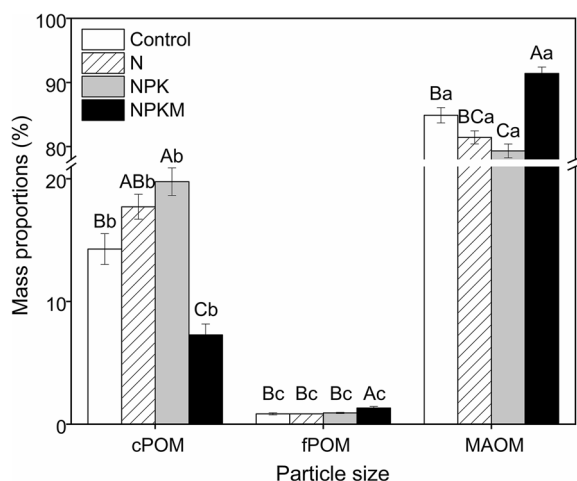


**Fig. 1** Mass distribution of the three physical size classes of SOM (coarse POM, fine POM, and mineral-associated OM) under four 32-year fertilization regimes: control (no fertilizer), N (urea), NPK (urea +  $\text{Ca}(\text{H}_2\text{PO}_4)_2$  + KCl), and NPKM (NPK + pig manure) in the Ferralic Cambisol. Uppercase letters indicate differences among fertilization types at  $p < 0.05$  level. Lowercase letters represent differences among the physical sizes at  $p < 0.05$  level

+10.6%, +14.2%, +23%, and +52%, respectively, in contrast to the initial status in 1986. The NPKM amendment had 36% more of total SOC content compared to control, mainly in the MAOM fraction (+48%) (Fig. 2a). Compared to the unfertilized control, the NPKM had lower SOC content in cPOM (−15%), but higher SOC content in fPOM (+145%). There was little change in TN content in the bulk soil among the four amendments (Fig. 2b). The NPK had higher TN content in cPOM (+75%), whereas the NPKM had more TN content in fPOM (+158%) compared with unfertilization. The NPKM amendment had higher C/N ratio in the bulk soil (+16%) and the MAOM fraction (+25%) (Fig. 2c). Among the fractions, the MAOM had much more SOC and TN than the POM. With the decrease in the size of physical fractions, C/N ratio decreased.

The 32-year total input-C were minimal under the unfertilized control ( $20.2 \text{ t C ha}^{-1}$ ) and maximal under the NPKM fertilization ( $160 \text{ t C ha}^{-1}$ ) (Table 1). There was a positive linear correlation between the SOC sequestration and total input-C (Fig. 3), with a conversion efficiency from the total input-C (plant residue and manure) to SOC of 6.8%.

### 3.3 Biochemical composition of organic amendments (residue and manure) and SOM

The straws from the control, NPK, and NPKM had similar biochemical compositions (Fig. 4a). Compared with the straw, however, the pig manure had more proportion of amino N-containing compounds and phenolics and

less relative abundance of lignin derivatives (Fig. 4a). In contrast, the straw and manure both had different biochemical composition patterns compared with the SOM (Figs. 4 and 5). Within the SOM, fertilization regime and particle sizes both shifted its biochemical composition, especially the proportions of N-bearing (amino, heterocyclic, and other) compounds and aromatics (Figs. 4 and 5). Fertilization mainly affected the proportions of other N-bearing compounds and lignin derivatives, while physical size influenced the monocyclic and polycyclic aromatics, lignins, and amino-N- and heterocyclic-N-bearing compounds (Fig. 4b and Table S1). The N fertilization reduced amino N-containing compounds in bulk soil (−32%) and MAOM (−36%) in contrast to the unfertilized control; whereas the NPK and NPKM amendments decreased other N-containing compounds in cPOM by −90% and −96%, respectively. The NPKM decreased the heterocyclic N-containing compounds in bulk soil (39%) and MAOM (42%) (Fig. 4b). Based on the variance partitioning analysis, the physical size classes and fertilizations explained 32% and 5% of the variation in SOM chemistry, respectively (Fig. S1 a), indicating the physical size classes was the primary factor (Fig. 5).

The proportions of polycyclic aromatics and N-containing compounds were both negatively correlated with the 32-year total C inputs, while the proportions of other compounds were positively correlated with the 32-year total input-C (Table S2).

### 3.4 Sources of SOM

Plant-derived compounds contributed 5–30% to whole SOM, and microbial-derived compounds contributed 60–90% to entire SOM under the four amendment regimes (Fig. 6). Physical size and fertilization regime both have less influence on the source of SOM (Fig. 7).

### 3.5 H/C, N/C, and O/C ratios and oxidation state

The MAOM fraction had higher atomic ratios of H/C and N/C than the POM fractions (Fig. 8a, b, d), while the fPOM had higher C oxidation states than both the cPOM and MAOM fractions (Fig. 8d–f). The cPOM fraction had lower atomic ratios of N/C and O/C (Fig. 8c). In contrast to the unfertilized control, the NPKM increased the O/C ratio of the fPOM (Fig. 8a, c, e). Physical size classes primarily affected the C oxidation state and O/C ratio rather than the various amendment regimes (Fig. 8, Table S1 and Fig. S1 b, c).

## 4 Discussion

### 4.1 SOM in physical fractions under long-term amendments

The MAOM fractions stored most of the SOC and TN (Fig. 2a, b) due to their highest mass portions ( $\geq 70\%$ )

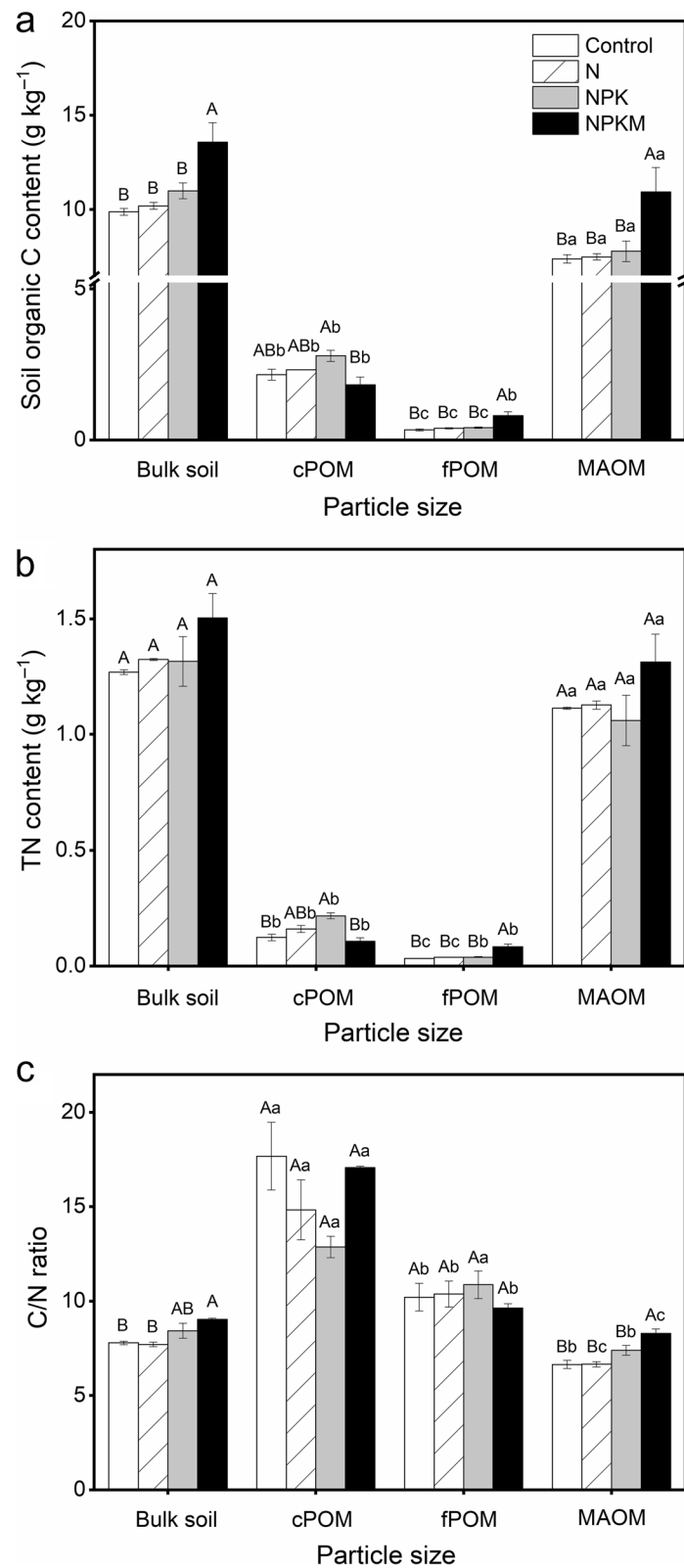


**Fig. 2** SOC and TN contents ( $\text{g kg}^{-1}$  bulk soil) and C/N ratio. Uppercase letters indicate differences among fertilization regimes at  $p < 0.05$  level. Lowercase letters suggest differences among the physical sizes at  $p < 0.05$  level

**Table 1** Estimates of 32-year cumulative C inputs ( $t C ha^{-1}$ ) into soils. Uppercase letters represent differences among the amendments at  $p < 0.05$  level

Fertilization regime	Root biomass C input	Composted manure C input	Total C input
Control	$20.2 \pm 0.33$ D	–	$20.2 \pm 0.33$ D
N	$26.2 \pm 0.37$ C	–	$26.2 \pm 0.37$ C
NPK	$45.0 \pm 0.67$ A	–	$45.06 \pm 0.67$ B
NPKM	$57.5 \pm 0.73$ B	102.5	$160.0 \pm 0.73$ A

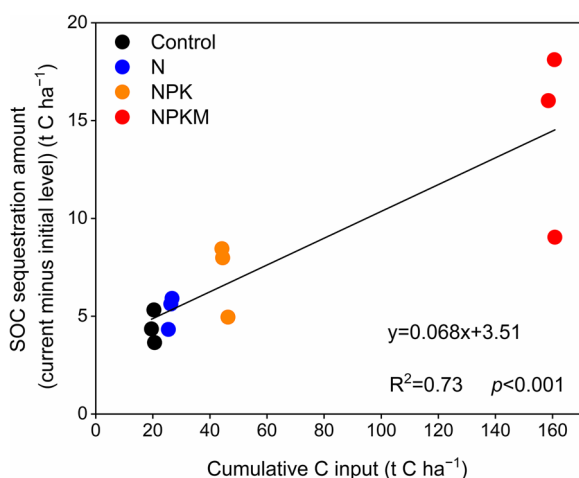


**Fig. 3** Linear regression relationship between 32-year total input-C and SOC sequestration in bulk soil

(Fig. 1; Christensen 2001; Wang et al. 2021) and higher persistence to microbial utilization in contrast to the other two fractions (von Lützw et al. 2007; Lavalée et al. 2020) and higher chemical affinities of Fe and Al oxy-hydroxides to SOM (Kleber et al. 2015; Guo et al. 2020; Kleber et al. 2021). Compared with the unfertilized control, mineral amendments had little influence on the SOC and TN (Fig. 2), which was mainly attributed to (i) the quite low conversion efficiency (6.8%) of input-OM to SOM and little change of root input rate under mineral fertilization, and (ii) the obvious atmospheric N deposition ( $> 25 kg N ha^{-1} yr^{-1}$ ) (Liu et al. 2010) to all fertilization treatments, which impaired the potential influence from the mineral N and NPK fertilizations. In contrast, manure amendment promoted the SOC content, especially for the MAOM fraction (Fig. 2a), which is beneficial for soil fertility and is consistent with many previous studies (e.g., Wang et al. 2015; Song et al. 2022a).

The positive linear relationship between the 32-year total input-C and SOC sequestration (Fig. 3) indicated that the studied upland red soils, even with large manure addition, did not reach SOC saturation, which should

be ascribed to the low conversion efficiency here (6.8%), similar to the soils in Xuzhou (7%) and Zhengzhou (6.9%) (Zhang et al. 2010). This low conversion efficiency might be attributed to the subtropical climate-induced faster rate of mineralization and higher degree of decomposition of SOM. Yet, several much higher conversion efficiencies (21–31%) were documented in other soils (Wang et al. 2015; Zhang et al. 2010), which might depend on various climatic conditions and soil parent materials. However, it was interesting that the SOC in cPOM was depressed by pig manuring, which was mainly due to the decrement of its mass proportions. Two potential explanations were proposed for this result: (i) the input pig manure was decomposed fast because of the subtropical warm and humid conditions, which might destroy partial water-stable macroaggregates (including Fe and Al oxy-hydroxides) that could not be broken by shaking; (ii) the employed wet sieving method here was inadequate to isolate the real cPOM from coarse sand and water-stable macroaggregates, and their mass proportions usually have strong spatial heterogeneity in nature soils. Therefore, for future studies, the density fractionation method is recommended to combine with physical size grouping approach to adequately separate the real cPOM from coarse mineral fractions. In contrast, despite of long-term N addition, the mineral and manure amendments all had little influence on the TN contents in the bulk soils and MAOM fractions (Fig. 2b), which might be attributed to the increments of production-induced N removal and high wet reactive N deposition background mentioned above (Liu et al. 2010). The cPOM had the highest C/N ratios whereas the MAOM had the lowest ones in all the four amendments (Fig. 2c), consistent with their proportions of microbial-derived compounds (Fig. 5), which supports the first hypothesis that fPOM should be the transitional component among the three physical sizes.

#### 4.2 Biochemical features of SOM

Long-term straw and manure amendments, with distinct biochemical features in contrast to SOM, had little impact on the biochemical properties of whole SOM as well as three fractions (Fig. 4), indicating the dominant reformation of input OM by soil microorganism (Kallenbach et al. 2016; Yan et al. 2022). Despite distinct qualities of input substrate, this convergence of most compounds might be attributed to the subtropical humid climate-induced high SOM decomposition degree and rate. In support, the majority of SOM was microbial-derived compounds (Fig. 6). It should be noticed that the enrichments of phenolic and lignin from pig manure were preserved in both the cPOM and fPOM fractions, not for the MAOM (Fig. 4a, b).



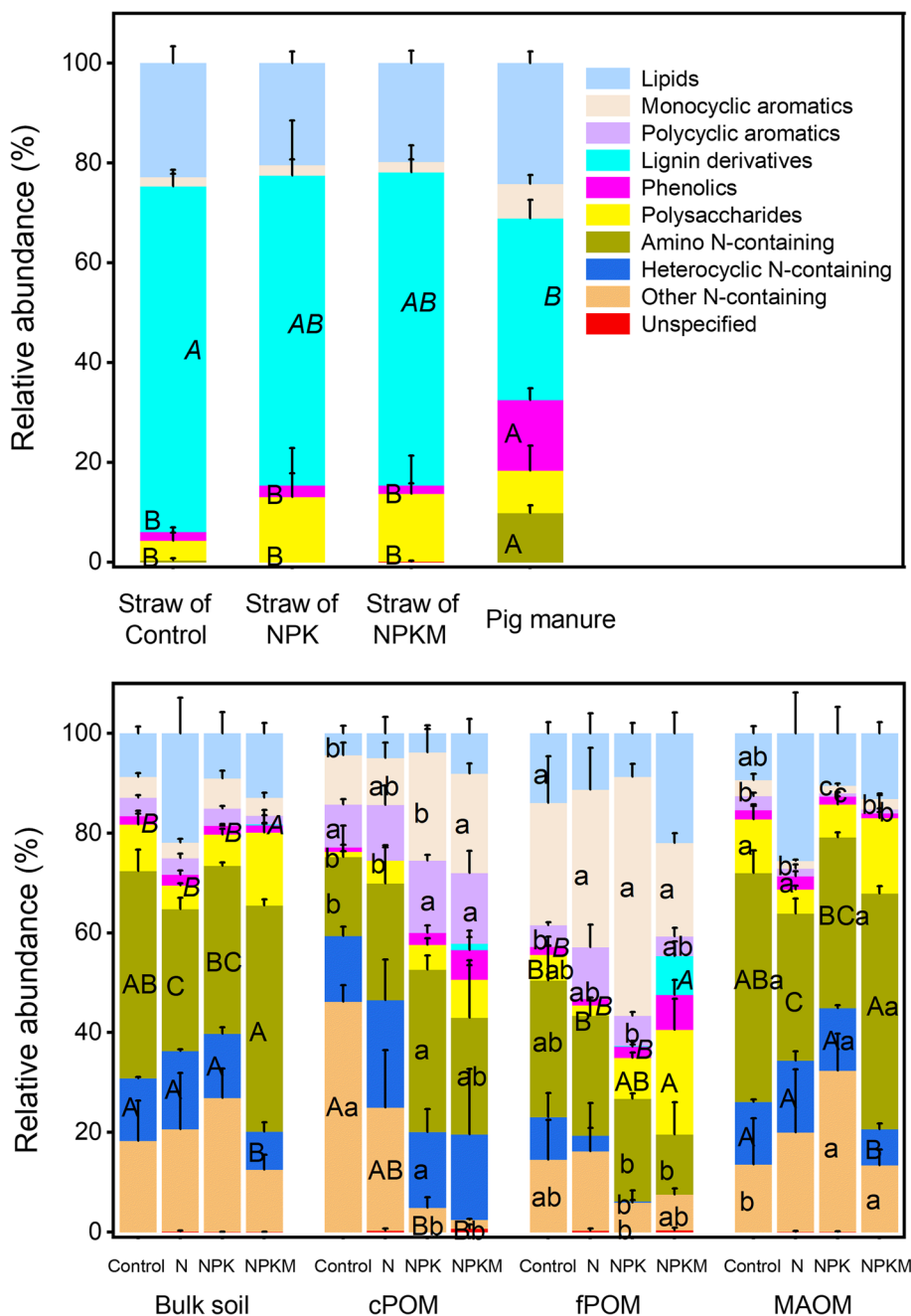


**Fig. 4** Biochemical composition (relative abundance) of straw and pig manure (a) and SOM (b). Uppercase letters indicate differences among fertilization regimes at  $p < 0.05$  level, in which italics are differences within lignin derivatives. Lowercase letters indicate differences among the physical sizes at  $p < 0.05$  level

However, the relative abundance of amino N-containing compound in pig manure was not transferred to the cPOM and fPOM under the NPKM amendment (Fig. 4a, b). There are two potential explanations for this result: (i) the enriched amino N-containing compound in manure was mainly derived from microbial processes during pig digestion (Kleber et al. 2007; Liang

et al. 2017); nevertheless (ii) the pig manure was not adequately decomposed because of its short-term, while the POM in soil experienced much longer and stronger microbial decomposition (Helfrich et al. 2006) especially under the subtropical warm and humid climate. Furthermore, mineral amendment had little impact on the proportions of entire N-containing compounds

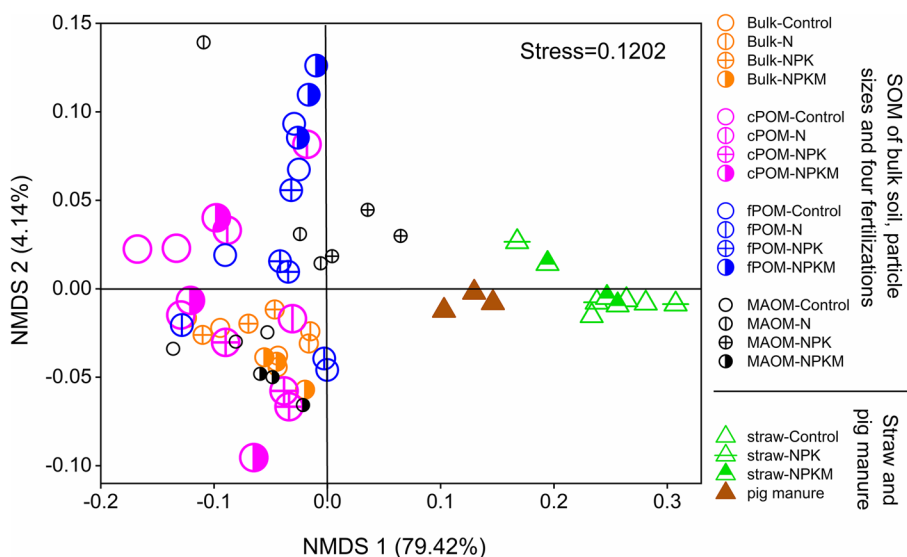


**Fig. 5** Non-metric multidimensional scaling (NMDS) analysis of the biochemical composition of straw, pig manure and SOM. The size of circle symbolically represents the physical size

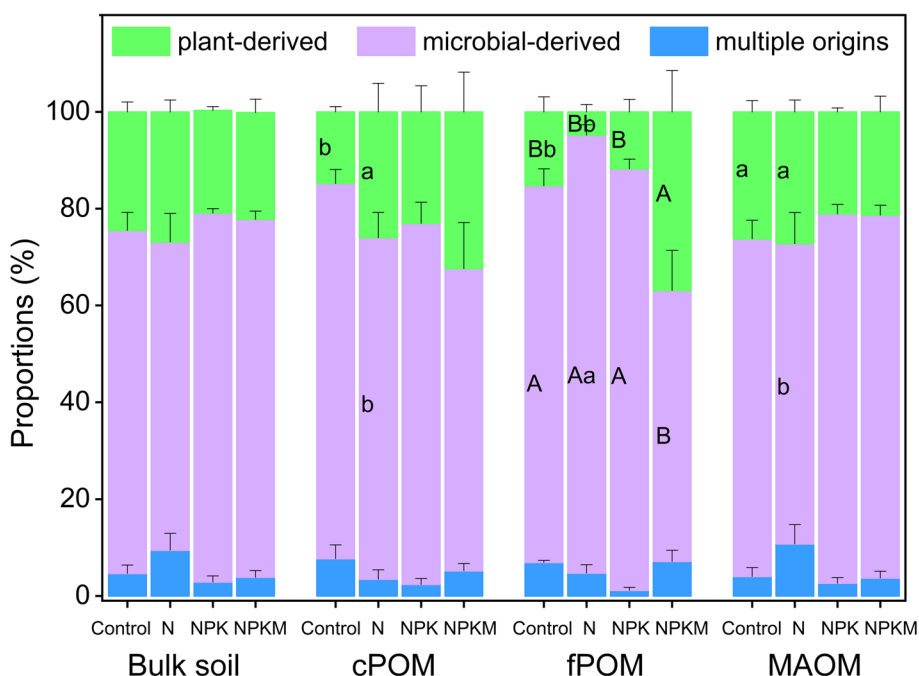


**Fig. 6** Sources of SOM: plant-derived, microbial-derived and multiple origins. Uppercase letters indicate differences among fertilization regimes at  $p < 0.05$  level. Lowercase letters represent differences among physical sizes at  $p < 0.05$  level

(amino + heterocyclic + other) (Fig. 4), which may be attributed to their similar contents of Fe and Al oxyhydroxides in this Ferralic Cambisol soil (Yu et al. 2020).

Physical size grouping resulted in a divergence trend in SOM biochemical compositions, with accumulation

of aromatics and lignin in the POM fractions and enrichment of N-bearing compounds in the MAOM fractions (Fig. 4), similar to previous results (Steffens et al. 2011; Rumpel et al. 2012). There are three explanations for this divergence phenomenon: (i) the physical sizes greatly represent the SOM decomposition

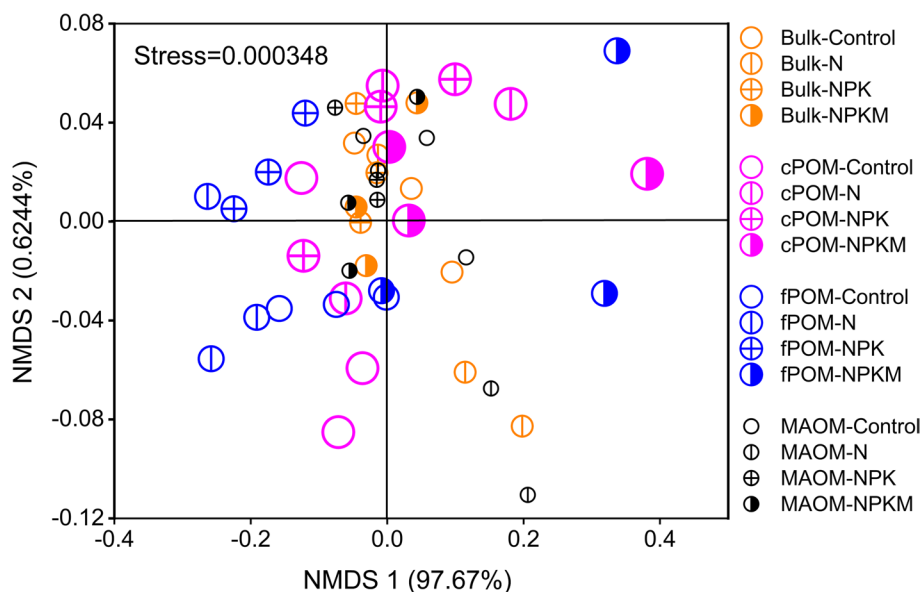


**Fig. 7** Non-metric multidimensional scaling (NMDS) analysis of three SOM sources. The size of circle symbolically represents the physical size

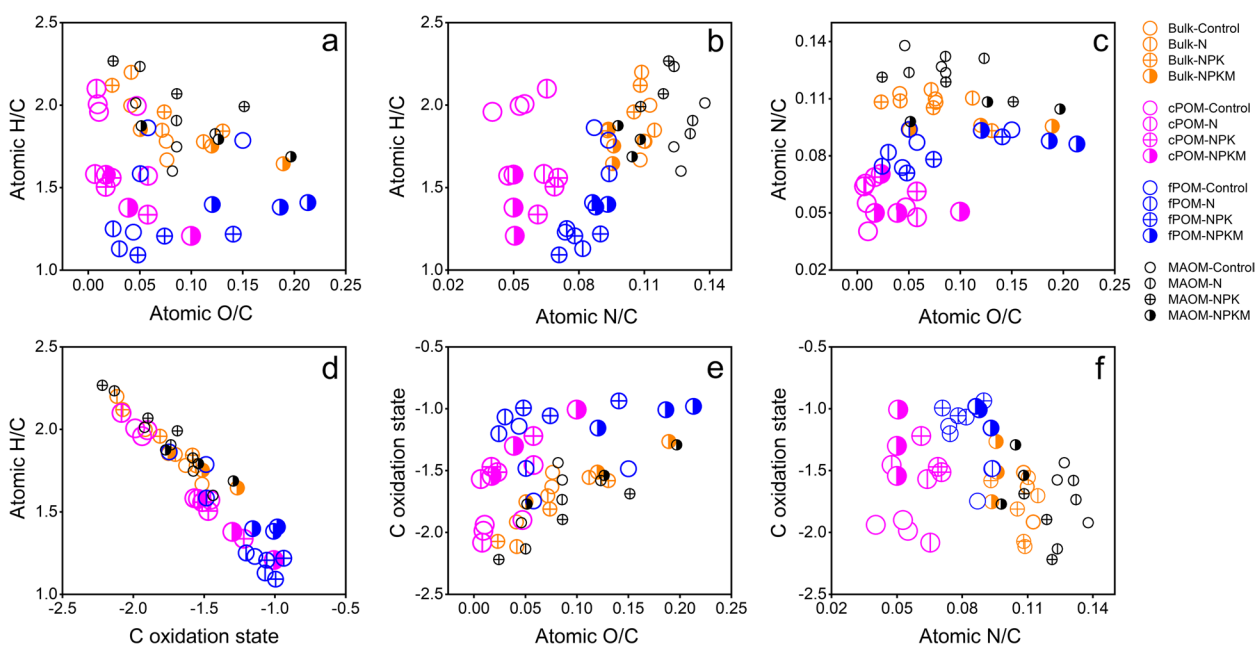


**Fig. 8** van Krevelen diagram of atomic ratios of H/C, O/C, and N/C and C oxidation state of SOM

degrees (von Lützw et al. 2007). So, it is reasonable that the recalcitrant compounds were retained relatively and selectively in the cPOM and fPOM fractions because of their short-term persistence (Kleber 2010); (ii) the fact that fPOM was partly occluded by microaggregates (Wang et al. 2017; Totsche et al. 2018; Wang et al. 2021), which can retain aromatics and lignin; and (iii) the N-containing compounds, largely derived

from microbial metabolites and necromass (Simpson et al. 2007; Creamer et al. 2019; Kopittke et al. 2020), can be easily and tightly adsorbed by minerals (especially Fe and Al oxy-hydroxides) (Kopittke et al. 2020; Kleber et al. 2021) and consequently persists for long-term in MAOM (organo-mineral associations) (Possinger et al. 2020; Kleber et al. 2021; Kögel-Knabner and Amelung 2021). The result showed that the physical

size primarily influenced the SOM biochemical composition, which supported the first hypothesis. However, there was no convergence trend in the chemistry of SOM across the physical size classes gradient (fPOM as the transitional fraction) (Figs. 4 and 5), which partly rejected the first hypothesis. This may be ascribed to (i) the offset of sand-associated OM to the real cPOM and (ii) the physical protection of partial fPOM by microaggregates (Wang et al. 2021).

Microbial-derived compounds contributed the majority of SOM under all amendments (Fig. 6), which was reasonable under such a warm and humid climate conditions (Yan et al. 2022) and consistent with those in temperate regions (e.g., Kögel-Knabner 2002; Mikutta et al. 2009; Barré et al. 2018). Physical size classes affected the O/C atomic ratio and C oxidation state, which was reduced more in cPOM and MAOM and oxidized more in fPOM, while lower H/C ratio was in fPOM (Fig. 8a, b, d, e). The SOM oxidation states ranged from  $-2.22$  to  $-0.94$ , with an average of  $-1.58$ , which was much lower than the values reported for both the Australian subtropical (an average of  $-0.3$ ) and Alaska boreal soils (a mean of  $-0.26$ ) (Hockaday et al. 2009). It is well known that the lower SOM oxidation state generally represents higher microbial vulnerability (Hockaday et al. 2009). Based on this principle, the cPOM and MAOM with lower SOM oxidation states (Fig. 8) were supposed to be easier to be decomposed by microorganisms rather than fPOM. It is reasonable that the cPOM is vulnerable to microbial decomposition. In reality, however, the MAOM generally has long-term persistence because of the physical protection (Lehmann and Kleber 2015; Kleber et al. 2021). Therefore, the potential microbial vulnerability of the MAOM can be amended for prolonged persistence through segregating microbial access.

Even though the Py-GC/MS is a useful technique for characterizing biochemical composition of SOM, it is not perfect. This technique has a drawback that it can not capture all compounds of SOM because of the incomplete pyrolysis effluents (Haddix et al. 2016). Furthermore, although the soils had passed through the 0.15-mm mesh, the clay minerals and Fe/Al oxides may act as catalysts which may influence the molecular composition resulting from pyrolysis.

## 5 Conclusions

The SOC contents and sequestrations were influenced by long-term fertilizations with a low conversion efficiency of 6.8%, while the biochemical compositions and C oxidation states of SOM were mostly modulated by

the physical size classes. The aromatics and lignins were enriched in the POM fractions (cPOM and fPOM), suggesting the relative selective retention of recalcitrant compounds. In contrast, the N-bearing compounds (particularly amino N) were accumulated in MAOM due to their high affinities to soil minerals. The fPOM was the most oxidized fraction while the cPOM and MAOM both reduced. Thus, physical size groups were able to separate SOM into biochemically different fractions under the long-term fertilizations. The result that both the fertilization and plant residues had weak effects on SOM biochemical features suggested that the physical fractionation (proxy of microbial decomposition degree) plays a more important role in regulating SOM chemistry than the initial quality of amendments.

### Abbreviations

BD	Bulk density
C/N	SOC/TN
cPOM	Coarse particulate organic matter
fPOM	Fine particulate organic matter
MAOM	Mineral-associated organic matter
Py-GC/MS	Pyrolysis-gas chromatography-mass spectrometry
NMDS	Non-metric multidimensional scaling
NPKM	NPK plus pig manure
SOC	Soil organic carbon
SOM	Soil organic matter
N	Urea
NPK	Urea plus $\text{Ca}(\text{H}_2\text{PO}_4)_2$ plus KCl
N/C, O/C and H/C	Atomic ratios of N/C, O/C and H/C, respectively
TN	Total N

### Supplementary Information

The online version contains supplementary material available at <https://doi.org/10.1007/s44246-022-00034-0>.

**Additional file 1: Table S1.** Two-way ANOVA of physical size classes and fertilization regime. **Table S2.** Linear regressions between cumulative C inputs (x) and the relative abundance of SOM compounds (y) (only significant related linear regressions were shown).

**Additional file 2: Fig. S1.** The variance partitioning analysis of biochemical composition, the atomic ratios of H/C and C oxidation state of SOM.

### Acknowledgements

Not applicable.

### Authors' contributions

YC: Formal analysis; Investigation; Literature collection and analysis; Writing-original draft. KLL: Investigation; Funding acquisition; Resources. NH: Writing-reviewing and editing. YLL: Conceptualization; Funding acquisition. FW: Writing-reviewing and editing. YDW: Conceptualization; Funding acquisition; Project administration; Supervision; Writing-reviewing and editing. All authors read and approved the final manuscript.

### Funding

This research was supported by the National Natural Science Foundation of China (31300381, 41201288 and 31570523) and the project of Double Thousand Plan in Jiangxi Province of China (jxsq2020102116).

### Availability of data and materials

The datasets used or analyzed during the current study are available from the corresponding author on reasonable request.

## Declarations

### Consent for publication

All authors declare that they are consent for publication in the journal of Carbon Research.

### Competing interests

All authors declare that there are no competing interests.

### Author details

<sup>1</sup>Tianjin Key Laboratory of Water Resources and Environment, & School of Geographic and Environmental Sciences, Tianjin Normal University, Tianjin 300387, China. <sup>2</sup>National Engineering and Technology Research Center for Red Soil Improvement, Jiangxi Institute of Red Soil, Nanchang 331717, China. <sup>3</sup>Department of Microbiology and Plant Biology, University of Oklahoma, Norman, OK 73019, USA. <sup>4</sup>Institute of Environment and Sustainable Development in Agriculture, Chinese Academy of Agricultural Sciences, Beijing 100081, China.

Received: 3 October 2022 Revised: 6 December 2022 Accepted: 27 December 2022

Published online: 11 January 2023

## References

- Angst G, Mueller KE, Klaas GJ, Nierop KGJ, Simpson MJ (2021) Plant- or microbial-derived? A review on the molecular composition of stabilized soil organic matter. *Soil Biol Biochem* 156:108189. <https://doi.org/10.1016/j.soilbio.2021.108189>
- Baldock JA, Skjemstad JO (2000) Role of the soil matrix and minerals in protecting natural organic materials against biological attack. *Org Geochem* 31:697–710. [https://doi.org/10.1016/S0146-6380\(00\)00049-8](https://doi.org/10.1016/S0146-6380(00)00049-8)
- Barré P, Quénéa K, Vidal A, Cécillon L, Christensen BT, Kätterer T, Macdonald A, Petit L, Plante AF, Oort F, Chenu C (2018) Microbial and plant-derived compounds both contribute to persistent soil organic carbon in temperate soils. *Biogeochemistry* 140:81–92. <https://doi.org/10.1007/s10533-018-0475-5>
- Becker JN, Dippold MA, Hemp A, Kuzyakov Y (2019) Ashes to ashes: characterization of organic matter in andosols along a 3400m elevation transect at Mount Kilimanjaro using analytical pyrolysis. *Catena* 180:271–281. <https://doi.org/10.1016/j.catena.2019.04.033>
- Bol R, Poirier N, Balesdent J, Gleixner G (2009) Molecular turnover time of soil organic matter in particle-size fractions of an arable soil. *Rapid Commun Mass Sp* 23:2551–2558. <https://doi.org/10.1002/rcm.4124>
- Cai Z, Yan X, Gu B (2022) Applying C:N ratio to assess the rationality of estimates of carbon sequestration in terrestrial ecosystems and nitrogen budgets. *Carbon Res* 1:2. <https://doi.org/10.1007/s44246-022-00004-6>
- Chen Q, Lei T, Wu Y, Si G, Xi C, Zhang G (2019) Comparison of soil organic matter transformation processes in different alpine ecosystems in the Qinghai-Tibet plateau. *J Geophys Res Biogeosci* 124:33–45. <https://doi.org/10.1029/2018JG004599>
- Christensen BT (2001) Physical fractionation of soil and structural and functional complexity in organic matter turnover. *Eur J Soil Sci* 52:345–353. <https://doi.org/10.1046/j.1365-2389.2001.00417.x>
- Cleveland CC, Liptzin D (2007) C:N:P stoichiometry in soil: is there a “Redfield ratio” for the microbial biomass? *Biogeochem* 85:235–252. <https://doi.org/10.1007/s10533-007-9132-0>
- Creamer CA, Foster AL, Lawrence C, McFarland J, Schulz M, Waldrop MP (2019) Mineralogy dictates the initial mechanism of microbial necromass association. *Geochim Cosmochim Acta* 260:161–176. <https://doi.org/10.1016/j.gca.2019.06.028>
- Gunina A, Smith AR, Kuzyakov Y, Jones DL (2017) Microbial uptake and utilization of low molecular weight organic substrates in soil depend on carbon oxidation state. *Biogeochemistry* 133:89–100. <https://doi.org/10.1007/s10533-017-0313-1>
- Guo S, Cai Y, Ren J, Guan Y, Xin D, Long X (2020) Formation and migration of magnetic particles associated with iron oxide transformation at a hillslope scale. *Catena* 197:104944. <https://doi.org/10.1016/j.catena.2020.104944>
- Haddix ML, Magrini-Bair K, Evans RJ, Conant RT, Wallenstein MD, Morris SJ et al (2016) Progressing towards more quantitative analytical pyrolysis of soil organic matter using molecular beam mass spectroscopy of whole soils and added standards. *Geoderma* 283:88–100. <https://doi.org/10.1016/j.geoderma.2016.07.027>
- Hammer Ø, Harper DAT, Ryan PD (2001) PAST: paleontological statistics software package for education and data analysis. *Palaeontol Electron* 4:1–9. <http://palaeo-electronica.org/20011/past/issue101.htm>
- Hasegawa S, Marshall J, Sparrman T, Näsholm T (2021) Decadal nitrogen addition alters chemical composition of soil organic matter in a boreal forest. *Geoderma* 386:114906. <https://doi.org/10.1016/j.geoderma.2020.114906>
- Helfrich M, Ludwig B, Buurman P, Flessa H (2006) Effect of land use on the composition of soil organic matter in density and aggregate fractions as revealed by solid-state C-13 NMR spectroscopy. *Geoderma* 136:331–341. <https://doi.org/10.1016/j.geoderma.2006.03.048>
- Hemingway JD, Rothman DH, Grant KE, Rosengard SZ, Eglinton TI, Derry LA, Galy VV (2019) Mineral protection regulates long-term global preservation of natural organic carbon. *Nature* 570:228–231. <https://doi.org/10.1038/s41586-019-1280-6>
- Hockaday WC, Masiello CA, Randerson JT, Smernik RJ, Baldock JA, Chadwick OA, Harden JW (2009) Measurement of soil carbon oxidation state and oxidative ratio by <sup>13</sup>C nuclear magnetic resonance. *J Geophys Res* 114:G02014. <https://doi.org/10.1029/2008JG000803>
- Kallenbach CM, Frey SD, Grandy AS (2016) Direct evidence for microbial-derived soil organic matter formation and its ecophysiological controls. *Nat Commun* 7:1–10. <https://doi.org/10.1038/ncomms13630>
- Kleber M (2010) What is recalcitrant soil organic matter? *Environ Chem* 7:320–332. <https://doi.org/10.1071/EN10006>
- Kleber M, Bourg IC, Coward EK, Hansel CM, Myneni SCB, Nunan N (2021) Dynamic interactions at the mineral–organic matter interface. *Nat Rev Earth Env* 2:402–421. <https://doi.org/10.1038/s43017-021-00162-y>
- Kleber M, Eusterhues K, Keiluweit M, Mikutta C, Mikutta R, Nico PS (2015) Mineral-organic associations: formation, properties, and relevance in soil environments. *Advances in Agronomy* 130: 1–140. <https://doi.org/10.1016/bs.agron.2014.10.005>
- Kleber M, Sollins P, Sutton R (2007) A conceptual model of organo-mineral interactions in soils: self-assembly of organic molecular fragments into zonal structures on mineral surfaces. *Biogeochemistry* 85:9–24. <https://doi.org/10.1007/s10533-007-9103-5>
- Kögel-Knabner I (2002) The macromolecular organic composition of plant and microbial residue as inputs to soil organic matter. *Soil Biol Biochem* 4:139–162. [https://doi.org/10.1016/S0038-0717\(01\)00158-4](https://doi.org/10.1016/S0038-0717(01)00158-4)
- Kögel-Knabner I, Amelung W (2021) Soil organic matter in major pedogenic soil groups. *Geoderma* 384:114785. <https://doi.org/10.1016/j.geoderma.2020.114785>
- Kögel-Knabner I, Guggenberger G, Kleber M, Kandeler E, Kalbitz K, Scheu S, Eusterhues K, Leinweber P (2008) Organo-mineral associations in temperate soils: integrating biology, mineralogy, and organic matter chemistry. *J Plant Nutr Soil Sci* 171:61–82. <https://doi.org/10.1002/jpln.200700048>
- Kopittke PM, Dalal RC, Hoeschen C, Li C, Menzies NW, Mueller CW (2020) Soil organic matter is stabilized by organo-mineral associations through two key processes: the role of the carbon to nitrogen ratio. *Geoderma* 357:1–9. <https://doi.org/10.1016/j.geoderma.2019.113974>
- Lavallee JM, Soong JL, Cotrufo MF (2020) Conceptualizing soil organic matter into particulate and mineral-associated forms to address global change in the 21st century. *Glob Change Biol* 26:261–273. <https://doi.org/10.1111/gcb.14859>
- Lehmann J, Kleber M (2015) The contentious nature of soil organic matter. *Nature* 528:60–68. <https://doi.org/10.1038/nature16069>
- Li SK, Tu HY, Zhang WF, Yang G (1992) The distribution of maize root in soil and its relation to aboveground. *Xinjiang Agri Sci* 2:99–103 (in Chinese with English abstract)
- Liang C, Schimel JP, Jastrow JD (2017) The importance of anabolism in microbial control over soil carbon storage. *Nat Microbiol* 2:1–6. <https://doi.org/10.1038/nmicrobiol.2017.105>
- Liu SQ, Song FB (2007) Comparative study on the characteristics of root system among maize genotypes with different tolerance to drought. *Journal of Yangzhou University (Agricultural Life Science Edit)* 28:68–74 (in Chinese with English abstract). <https://doi.org/10.16872/j.cnki.1671-4652.2007.01.016>



- Liu X, Song L, He C, Zhang F (2010) Nitrogen deposition as an important nutrient from the environment and its impact on ecosystems in China. *Journal of Arid Land* 2:137–143. <https://doi.org/10.3724/SP.J.1227.2010.00137>
- Lützwalt MV, Kögel-Knabner I, Ekschmitt K, Flessa H, Guggenberger G, Matzner E, Marschner B (2007) SOM fractionation methods: relevance to functional pools and to stabilization mechanisms. *Soil Biol Biochem* 39:2183–2207. <https://doi.org/10.1016/j.soilbio.2007.03.007>
- Mikutta R, Schaumann GE, Gildemeister D, Bonneville S, Kramer MG, Chorover J, Chadwick OA, Guggenberger G (2009) Biogeochemistry of mineral-organic associations across a long-term mineral soil gradient (0.3–4100 kyr), Hawaiian islands. *Geochim Cosmochim Acta* 73:2034–2060. <https://doi.org/10.1016/j.gca.2008.12.028>
- Pascaud G, Soubrand M, Lemeé L, Laduranty J, El-Mufleh A, Rabiet M, Joussein E (2017) Molecular fingerprint of soil organic matter as an indicator of pedogenesis processes in Technosols. *J Soils Sediments* 17:340–351. <https://doi.org/10.1007/s11368-016-1523-1>
- Paul EA (2016) The nature and dynamics of soil organic matter: plant inputs, microbial transformations, and organic matter stabilization. *Soil Biol Biochem* 98:109–126. <https://doi.org/10.1016/j.soilbio.2016.04.001>
- Possinger AR, Zachman MJ, Enders A, Levin BDA, Muller DA, Kourkoutis LF, Lehmann J (2020) Organo-organic and organo-mineral interfaces in soil at the nanometer scale. *Nat Commun* 11:6103. <https://doi.org/10.1038/s41467-020-19792-9>
- Rumpel C, Rodríguez-Rodríguez A, González-Pérez JA, Arbelo C, Chabbi A, Nunan N, González-Vila FJ (2012) Contrasting composition of free and mineral-bound organic matter in top- and subsoil horizons of andosols. *Biol Fertil Soils* 48:401–411. <https://doi.org/10.1007/s00374-011-0635-4>
- Schellekens J, Buurman P, Kalbitz K, Zomer AV, Vidal-Torrado P, Cerli C, Comans RNJ (2017) Molecular features of humic acids and fulvic acids from contrasting environments. *Environ Sci Technol* 51:1330–1339. <https://doi.org/10.1021/acs.est.6b03925>
- Schmidt MWI, Torn MS, Abiven S, Dittmar T, Guggenberger G, Janssens IA, Kleber M, Kögel-Knabner I, Lehmann J, Manning DAC, Nannipieri P, Rasse DP, Weiner S, Trumbore SE (2011) Persistence of soil organic matter as an ecosystem property. *Nature* 478:49–56. <https://doi.org/10.1038/nature10386>
- Schulten HR, Schnitzer M (1997) The chemistry of soil organic nitrogen: a review. *Biol Fertil Soils* 26:1–15. <https://doi.org/10.1007/s003740050335>
- Schweizer SA, Mueller CW, Hoschen C, Ivanov P, Kögel-Knabner I (2021) The role of clay content and mineral surface area for soil organic carbon storage in an arable toposequence. *Biogeochemistry* 156:401–420. <https://doi.org/10.1007/s10533-021-00850-3>
- Shah SAA, Xu M, Abrar MM, Mustafa A, Fahad S, Shah T, Shah SAA, Yang X, Zhou W, Zhang S, Nan S, Shi W (2021) Long-term fertilization affects functional soil organic carbon protection mechanisms in a profile of Chinese loess plateau soil. *Chemosphere* 267:128897. <https://doi.org/10.1016/j.chemosphere.2020.128897>
- Simpson AJ, Simpson MJ, Smith E, Kelleher BP (2007) Microbially derived inputs to soil organic matter: are current estimates too low? *Environ Sci Technol* 41:1–6. <https://doi.org/10.1021/es071217x>
- Six J, Elliott ET, Paustian K (2000) Soil macroaggregate turnover and microaggregate formation: a mechanism for C sequestration under no-tillage agriculture. *Soil Biol Biochem* 32:2099–2103. [https://doi.org/10.1016/S0038-0717\(00\)00179-6](https://doi.org/10.1016/S0038-0717(00)00179-6)
- Sokol NW, Bradford MA (2019) Microbial formation of stable soil carbon is more efficient from belowground than aboveground input. *Nat Geosci* 12:46–53. <https://doi.org/10.1038/s41561-018-0258-6>
- Song F, Liu K, Lou Y, Kuzyakov Y, Wang Y (2022a) Divergent responses of aggregate stability to long-term mineral and organic amendments between upland and paddy soils. *J Soils Sediments*. <https://doi.org/10.1007/s11368-022-03270-4>
- Song X, Wang P, Van Zwielen L, Bolan N, Wang H, Li X, Cheng K, Yang Y, Wang M, Liu T, Li F (2022b) Towards a better understanding of the role of Fe cycling in soil for carbon stabilization and degradation. *Carbon Res* 1:5. <https://doi.org/10.1007/s44246-022-00008-2>
- Steffens M, Kolbl A, Schork E, Gschrey B, Kögel-Knabner I (2011) Distribution of soil organic matter between fractions and aggregate size classes in grazed semiarid steppe soil profiles. *Plant Soil* 338:63–81. <https://doi.org/10.1007/s11104-010-0594-9>
- Stewart CE, Neff JC, Amatangelo KL, Vitousek PM (2011) Vegetation effects on soil organic matter chemistry of aggregate fractions in a Hawaiian forest. *Ecosystems* 14:382–397. <https://doi.org/10.1007/s10021-011-9417-y>
- Totsche KU, Amelung W, Gerzabek MH, Guggenberger G, Klumpp E, Knief C, Lehdorff E, Mikutta R, Peth S, Prechtel A, Ray N, Kögel-Knabner I (2018) Microaggregates in soils. *J Plant Nutr Soil Sci* 181:104–136
- Wang Y, Hu N, Ge T, Kuzyakov Y, Wang Z-L, Li Z, Tang Z, Chen Y, Wu C, Lou Y (2017) Soil aggregation regulates distributions of carbon, microbial community and enzyme activities after 23-year manure amendment. *Appl Soil Ecol* 111:65–72
- Wang Y, Hu N, Xu M, Li Z, Lou Y, Chen Y, Wu C, Wang Z-L (2015) 23-year manure and fertilizer application increases soil organic carbon sequestration of a rice-barley cropping system. *Biol Fertil Soils* 51:583–591. <https://doi.org/10.1007/s00374-015-1007-2>
- Wang Y, Wang Z-L, Zhang Q, Hu N, Li Z, Lou Y, Li Y, Xue D, Chen Y, Wu C, Zou CB, Kuzyakov Y (2018) Long-term effects of nitrogen fertilization on aggregation and localization of carbon, nitrogen and microbial activities in soil. *Sci Total Environ* 624:1131–1139. <https://doi.org/10.1016/j.scitotenv.2017.12.113>
- Wang Y, Xue D, Hu N, Lou Y, Zhang Q, Zhang L, Zhu P, Gao H, Zhang S, Zhang H, Li D, Song Z, Kurganova I, Kuzyakov Y, Wang Z-L (2021) Post-agricultural restoration of soil organic carbon pools across a climate gradient. *Catena* 200:105138. <https://doi.org/10.1016/j.catena.2020.105138>
- Yan M, Zhang X, Liu K, Lou Y, Wang Y (2022) Particle size primarily shifts chemical composition of organic matter under long-term fertilization in paddy soil. *Eur J Soil Sci* 73:e13170. <https://doi.org/10.1111/ejss.13170>
- Yang F, Tian J, Fang H, Gao Y, Xu M, Lou Y, Zhou B, Kuzyakov Y (2019) Functional soil organic matter fractions, microbial community, and enzyme activities in a Mollisol under 35 years manure and mineral fertilization. *J Soil Sci Plant Nut* 19:430–439
- Yang F, Tian J, Meersmans J, Fang H, Yang H, Lou Y, Li Z, Liu K, Zhou Y, Blagodatskaya E, Kuzyakov Y (2018) Functional soil organic matter fractions in response to long-term fertilization in upland and paddy systems in South China. *Catena* 162:270–277. <https://doi.org/10.1016/j.catena.2017.11.004>
- Yu G, Chen C, He X, Zhang X, Li L (2020) Unexpected bulk density and microstructures response to long-term pig manure application in a Ferralic Cambisol soil: implications for rebuilding a healthy soil. *Soil Till Res* 203:104668. <https://doi.org/10.1016/j.still.2020.104668>
- Zhang W, Liu K, Wang J, Shao X, Xu M, Li J, Wang X, Murphy DV (2015) Relative contribution of maize and external manure amendment to soil carbon sequestration in a long-term intensive maize cropping system. *Sci Rep* 5:1–12. <https://doi.org/10.1038/srep10791>
- Zhang W, Wang X, Xu M, Huang S, Liu H, Peng C (2010) Soil organic carbon dynamics under long-term fertilizations in arable land of northern China. *Biogeosciences* 7:409–425. <https://doi.org/10.5194/bg-7-409-2010>

## Publisher's Note

Springer Nature remains neutral with regard to jurisdictional claims in published maps and institutional affiliations.